Applied Physics Letters

Thickness-dependent ultrafast nonlinear absorption properties of $PtSe_2$ films with both semiconducting and semimetallic phases

Cite as: Appl. Phys. Lett. **115**, 263102 (2019); https://doi.org/10.1063/1.5135375
Submitted: 06 November 2019 . Accepted: 11 December 2019 . Published Online: 26 December 2019

Xin Zhao, Fang Liu, Dongqi Liu, Xiao-Qing Yan, Changfu Huo, Wangwei Hui, Junfang Xie, Qing Ye, Chengcheng Guo, Yang Yao, Zhi-Bo Liu, and Jian-Guo Tian

Applied Physics Letters ARTICLE scitation.org/journal/apl

Thickness-dependent ultrafast nonlinear absorption properties of $PtSe_2$ films with both semiconducting and semimetallic phases

Cite as: Appl. Phys. Lett. **115**, 263102 (2019); doi: 10.1063/1.5135375
Submitted: 6 November 2019 · Accepted: 11 December 2019 ·
Published Online: 26 December 2019

Xin Zhao,[1,2,a)] Fang Liu,[1,a)] Dongqi Liu,[1] Xiao-Qing Yan,[1,3,b)] Changfu Huo,[1] Wangwei Hui,[1] Junfang Xie,[1] Qing Ye,[1] Chengcheng Guo,[4] Yang Yao,[4] Zhi-Bo Liu,[1] and Jian-Guo Tian[1,3]

AFFILIATIONS

[1]Key Laboratory of Weak-Light Nonlinear Photonics, Ministry of Education, School of Physics, Nankai University, Tianjin 300071, China
[2]School of Physical Science and Technology, Tiangong University, Tianjin 300387, China
[3]Collaborative Innovation Center of Extreme Optics, Shanxi University, Taiyuan, Shanxi 030006, China
[4]Department of Neurology, Tianjin first center Hospital, No. 24 Fukang Rd. Tianjin 300192, China

[a)]**Contributions:** X. Zhao and F. Liu contributed equally to this work.
[b)]**Electronic mail:** yanxq01@nankai.edu.cn

ABSTRACT

The bandgap, electrical, and optical properties of $PtSe_2$ depend dramatically on the vertical stacking and fabrication method. Here, we study the nonlinear absorption properties of the $PtSe_2$ films composed of both semiconducting and semimetallic phases in a single film. These $PtSe_2$ films exhibit remarkable thickness-dependent saturable absorption for femtosecond pulses at 400 nm and 800 nm. The saturation intensities decrease with the increase in the film thickness due to the accompanied increase in the semimetallic component and are much smaller than the reported values of $PtSe_2$ synthesized by thermally assisted conversion. The saturable absorption characteristics are confirmed by time-resolved spectroscopies. The nonlinear refractive indexes of these $PtSe_2$ films should be smaller than 1×10^{-12} cm^2/W. Our results imply that the optical nonlinearities of $PtSe_2$ could be flexibly tuned by the synthesis method and thickness.

Published by AIP Publishing. https://doi.org/10.1063/1.5135375

The applications of 2D materials in optoelectronics and photonics require good knowledge on their ultrafast nonlinear optical (NLO) response since NLO effects are the physical basis.[1–4] The studies on the NLO properties of 2D materials are at the forefront of the present research activities.[5–7] $PtSe_2$ is such a 2D material that its bandgap dramatically depends on the vertical stacking due to the very strong interlayer coupling, leading to a semimetal-semiconductor transition when going from bulk to monolayer form.[8,9] However, the measured bandgap, electrical, and optical properties of $PtSe_2$ films synthesized by different methods are inconsistent.[8–14] For instance, the electrical transport characterization shows that 13 nm-thick mechanically exfoliated $PtSe_2$ exhibits metallic behavior;[9] however, thermally assisted conversion (TAC)-fabricated thick $PtSe_2$ layers (up to 30 nm-thick) exhibit semiconducting behavior.[11,12] Bandgap deviations do exist between theoretical values and experimental values.[8–10,15,16] The inconsistencies indicate the large variation in the properties of $PtSe_2$ and provide intensive motivation to explore the physical properties of $PtSe_2$ fabricated by different methods.

The ultrafast nonlinear absorption (NLA) of $PtSe_2$ synthesized by TAC has been reported.[16–18] These TAC-synthesized $PtSe_2$ films exhibit a single phase (semiconducting vs semimetallic) in a single film.[16–19] The NLA of $PtSe_2$ fabricated by other methods has not been investigated yet. Since the $PtSe_2$ bandgap greatly depends on the fabrication method,[8,10,18,20,21] it is inferred that the NLA of $PtSe_2$ should vary with the synthesis method. A specific study on the ultrafast NLA of $PtSe_2$ films grown by the direct chemical vapor deposition (CVD) method is necessary and is important for the application of such $PtSe_2$ films in photonic devices. In this work, we study the ultrafast NLA of the $PtSe_2$ films having both semiconducting and semimetallic phases in a single film. These direct CVD-grown $PtSe_2$ films exhibit significant thickness-dependent saturable absorption (SA) for femtosecond (fs) pulses at 400 nm and 800 nm due to the increase in the semimetallic content with the thickness and possessing smaller

TABLE I. Thickness of the $PtSe_2$ films.

$PtSe_2$ sample	A	B	C	D	E	F
Thickness (nm)	2.0	3.5	4.5	5.4	6.2	7.9
Layer number	3	5	6	8	9	11

saturation intensity and nonlinear refraction as compared with the TAC-synthesized $PtSe_2$.

Large-scale continuous $PtSe_2$ films with different thicknesses were directly grown on a quartz substrate via the CVD method (see S1 in the supplementary material). The optical microscopic and AFM images manifest the good homogeneity of the as-grown $PtSe_2$ films. The film thickness was determined from AFM measurements (Table I). The chemical state of elements was determined by X-ray photoelectron spectroscopy, which confirms the synthesis of $PtSe_2$. The Se:Pt stoichiometric ratios n_{Se}/n_{Pt} are determined to be 2.25 ± 0.05 for these films, implying the complete selenization and p-type doping in these films. Raman spectra indicate that these $PtSe_2$ films have a similar crystal structure to those fabricated by other methods (see S2 in the supplementary material).[8,21]

Figures 1(a)–1(f) show the source-drain current I_{DS} as a function of the applied back-gate voltage V_g from the field-effect transistors of these films. For all the films, the conductance could be modulated by the gate voltage, showing a p-type semiconducting transport property.[9] Figure 1(g) shows the thickness-dependent optical absorption spectra, which have been extended to 3300 nm. In all the films, we could observe a broadband absorption response with a smooth absorption band over a wide wavelength range from ~400 to ~800 nm, and then the absorption intensity decreases with the increase in the wavelength. As the films get thicker, red shifts in the absorption bands are seen. Then, the (nominal) optical bandgaps were extracted from the optical absorption spectra [Fig. 1(h) and see S3 in the supplementary material]. The extracted bandgap decreases with the film thickness and locates in the range from 0.97 to 0.57 eV

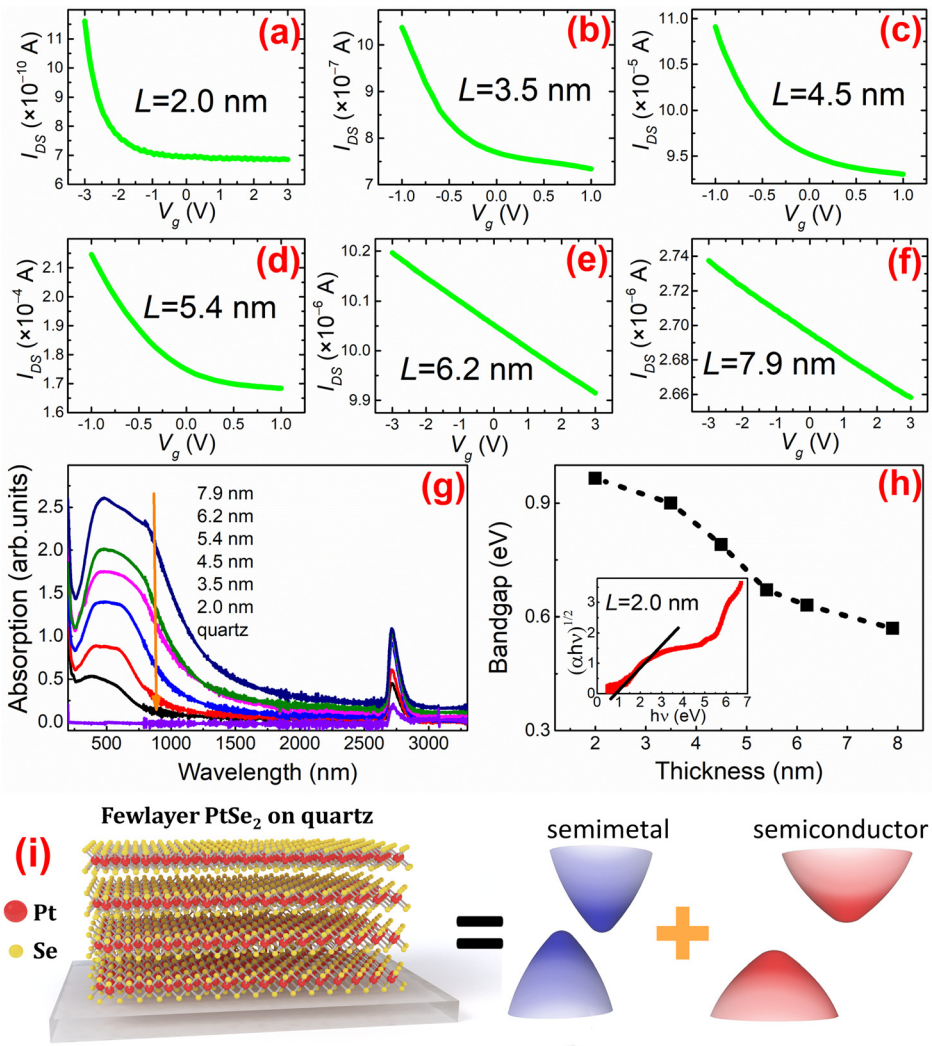

FIG. 1. (a)–(f) $I_{DS} - V_g$ curves ($V_{DS} = 1$ V) of field-effect transistors with different-thickness $PtSe_2$ films. (g) Absorption spectra of $PtSe_2$ films and the quartz substrate; the absorption peaks at 2715 nm come from the substrate. (h) Thickness-dependent bandgap of the $PtSe_2$ film; the inset shows the plot of $\sqrt{\alpha h\nu}$ vs $h\nu$ for sample A. (i) Illustration of the components of these $PtSe_2$ films.

(i.e., 1278–2175 nm). For each $PtSe_2$ film, there should be no absorption for light with photon energy much smaller than the bandgap.[8] However, we could observe weak optical absorption in the wavelength range extended to at least 3300 nm (0.376 eV) for these films. Therefore, the extracted bandgaps are invalid and a semimetallic phase should also exist [Fig. 1(i)].[20] It is known that the IR absorption of the metal film with the thickness on the order of percolation threshold deviates greatly from the Drude-model.[22,23] The IR absorption of these $PtSe_2$ films is similar to that of the 6.8 nm-thick Au film[23] and mainly comes from the semimetallic components of the films. The increase in IR absorption with the film thickness indicates the accompanied increase in the semimetallic component, which is in accordance with the weaker gate-modulation for the thicker $PtSe_2$ film. In contrast to $PtSe_2$ fabricated by either mechanical exfoliation or TAC,[8,9,16,18] the direct CVD-grown $PtSe_2$ films are composed of both semiconducting and semimetallic phases in a single film [Fig. 1(i)]. Since the phase relates to the crystal structure of material, the two phases should correspond to different structures in one $PtSe_2$ film. Thus, a slight structure change occurs in one $PtSe_2$ film. The detailed formation and distribution of both components/phases in such a thin film need further investigation, which is beyond the scope of this paper.

Following this, open-aperture (OA) Z-scan and time-resolved degenerate pump-probe ΔT/T spectroscopy were used to explore the NLA properties of these $PtSe_2$ films. A regenerative amplified fs Ti:sapphire laser system (Spitfire Pro) was used to generate fs pulses (center wavelength of 800 nm; repetition rate of 1 kHz). The fundamental pulse (800 nm) and its second harmonic generation (400 nm) were used in the measurements (see S4 in the supplementary material). We did not observe any NLA response from the substrate, and no laser-induced sample damage was observed in the measurements (the damage threshold of these $PtSe_2$ films should be larger than 3.1 mJ/cm^2 and 12.2 mJ/cm^2 for 800 nm and 400 nm pulses, respectively).

First, the NLA properties were measured by 800 nm pulses ($\tau_{FWHM} = 330$ fs). As shown in Fig. 2(a), the normalized transmittances of samples B-F increase monotonously as the sample is moved to the focus, indicating SA behavior in samples B-F. The SA signal intensity increases rapidly with the film thickness. The flat Z-scan trace of sample A ($L \approx 2.0$ nm) reflects that the NLA of sample A should be extremely small. In addition, the normalized transmittance monotonously increases with the pulse energy [e.g., Fig. 2(b) for sample F], which means that no multiphoton absorption simultaneously occurs in the measured energy range.[18,24]

The saturation intensity I_S could be calculated from the Z-scan trace fitting by accounting the intensity attenuation of the SA model $\frac{dI(Z,r,t)}{dz'} = -\frac{\alpha_0 I(Z,r,t)}{1+I(Z,r,t)/I_S}$ (see S5 in the supplementary material). The extracted I_S values are shown in Fig. 3(a). The decrease in I_S for thicker films suggests easier absorption saturation behavior for thicker $PtSe_2$ films. For the thin films ($L = 3.5$, 4.5, and 5.4 nm), the I_S values have no definite change as the incident pulse energy increases. For the thicker films ($L = 6.2$ and 7.9 nm), the I_S values decrease slightly with the increase in the pulse energy. The extracted I_S of sample F is about 5 GW/cm^2, comparable to those of bilayer graphene (~4 GW/cm^2) and the MoS_2 nanoplatelet film (1.85 GW/cm^2).[25–27] The Z-scan measurements at different sample positions give rise to the variation of less than 6% in the peak value of normalized transmittance due to the good homogeneity over a large scale. The variation of the I_S value should be within 8% for different sample positions.

To get some insight into the SA characteristics, degenerate 800 nm pump-probe measurements were performed. The schematic setup used here was similar to that in Ref. 28. The beam sizes of the pump and probe at the samples were ~80 μm and 35 μm, respectively. As shown in Figs. 4(a)–4(f), a pump-induced transmission enhancement could be observed around 0 delay time for these films, confirming the SA at 800 nm for samples B-F. For sample A, the positive ΔT/T signal around 0 delay time is extremely small and is immediately transited to negative (i.e., absorption enhancement). Therefore, the NLA of sample A should be negligible, which is consistent with the Z-scan result. For samples A–C, the initial SA response is followed by a photoinduced absorption process, which results in the negative ΔT/T. Since the NLA properties of materials are generally concerned for a single beam, the transient optical response after pump excitation could not influence the NLA properties measured with low-repetition-rate pulses (no more than 1 kHz). Thus, the negative ΔT/T after 500 fs could not give rise to reverse SA for samples A–C. In addition, the peak ΔT/T signal around 0 delay time increases with the film thickness, leading to more pronounced SA in the thicker $PtSe_2$ film.

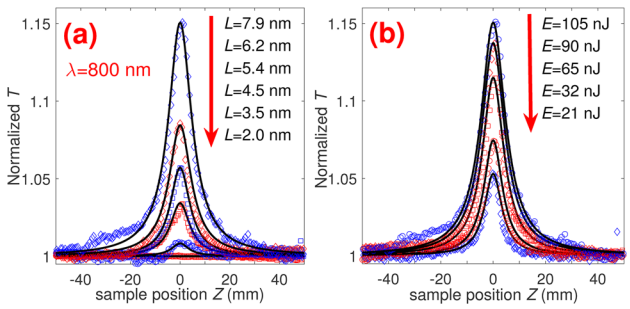

FIG. 2. OA Z-scan results with 800 nm pulses. (a) Z-scan traces at an incident energy of 105 nJ. (b) Z-scan traces of sample F ($L = 7.9$ nm) at different pulse energies. The scatters are experimental data and the solid lines show the theoretical fits.

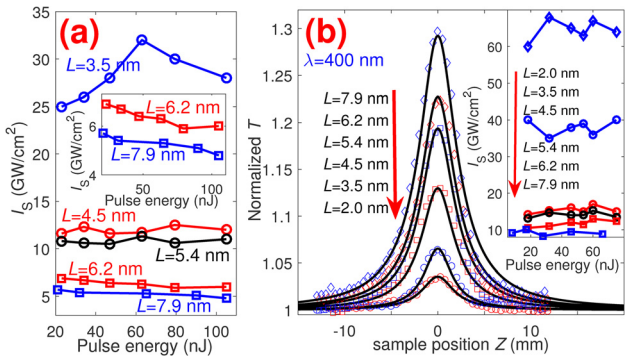

FIG. 3. (a) The dependence of I_S on the incident energy of the 800 nm pulse. Inset: The zoom-in view for samples E and F. (b) Thickness-dependent Z-scan traces under an excitation of 400 nm pulses with a pulse energy of 46 nJ. Inset: the dependence of I_S on the pulse energy of 400 nm.

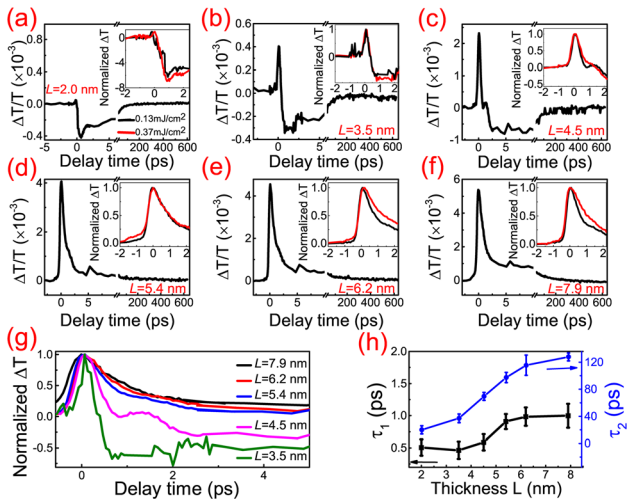

FIG. 4. (a)–(f) Time-resolved degenerate 800 nm pump-probe ΔT/T spectroscopies of $PtSe_2$ films. The pump fluences were 0.13 mJ/cm^2 (black line) and 0.37 mJ/cm^2 (red line). The insets illustrate the normalized ΔT traces around 0 delay time. (g) Thickness-dependent normalized ΔT traces of these films. (h) The variation of time constants with the film thickness.

The insets of Figs. 4(a)–4(f) show the normalized ΔT traces at different pump fluences. For the thin $PtSe_2$ films ($L = 2.0$–5.4 nm), the normalized ΔT traces have no visible variation in the positive ΔT/T region as the incident pulse energy increases, indicating that the initial carrier relaxation rate is independent of the pump fluence. However, for the two thicker films ($L = 6.2$ nm and 7.9 nm), the normalized ΔT signal is with a slower decay process for a larger pump fluence, which may be caused by the hot phonon effect and reflects a slower carrier relaxation rate at higher photoexcited carrier density.[29] The SA comes from the absorption coefficient reduction due to the state-filling effect (i.e., the photoexcited carriers block the corresponding interband transition, further resulting in the absorption reduction).[25] A slower carrier relaxation rate leads to that the nonequilibrium carriers remain at the probed energy state for longer time, giving rise to a stronger state-filling effect, further resulting in a more pronounced SA effect.[25] Thus, owing to the decrease in the initial carrier relaxation rate with the increase in the pump fluence, the I_S values of samples E and F show a slight decrease as the pump fluence increases.

Figure 4(g) summarizes the normalized ΔT traces of these samples; it is found that the ΔT/T signal relaxes slower for the thicker film. The slower relaxation rate results in a stronger state-filling effect and further leads to the decrease in I_S as the film thickness increases, which is in accordance with the Z-scan results.

The ΔT/T signal beyond 500 fs delay can be fit to a biexponential function, and the extracted time constants τ_1 and τ_2 increase as the film thickness increases [Fig. 4(h)]. Three thickness-dependent time constants (corresponding to the carrier-phonon scattering process, $\tau_c = 0.52$–1.29 ps, bandgap renormalization $\tau_{BGR} = 1.54$–2.63 ps, and electron-hole recombination $\tau_r = 81.2$–316.4 ps) have been observed in the TAC-fabricated semiconducting $PtSe_2$ films.[16] As compared with the TAC-fabricated $PtSe_2$ film with a similar thickness, the two time constants are smaller.[16] The difference should be caused by the different component in the two types of $PtSe_2$ films. According to the carrier relaxation process in TAC-fabricated $PtSe_2$ films, the time constants τ_1 and τ_2 may correspond to the bandgap renormalization and electron-hole recombination, respectively.[16] Since the measured ΔT/T signal comes from both semiconducting and semimetallic contents here, it is insufficient to extract the detailed carrier relaxation mechanisms from the two time constants. It is inferred that the carrier transfer between semiconducting and semimetallic contents should be one relaxation process[30] in addition to the bandgap renormalization and carrier recombination.[16] Owing to the indirect bandgap of $PtSe_2$, carrier recombination via light emission could be excluded, which has been confirmed by the no photoluminescence in these films. Carrier-carrier scattering and carrier-phonon scattering are two important carrier relaxation pathways.[30] Carrier-carrier scattering should dominate the initial thermalization process, and carrier-phonon scattering should be the dominant energy dissipation pathway of nonequilibrium carriers.

We now turn to the NLA of $PtSe_2$ films in the short wavelength region by performing measurements with 400 nm pulses ($\tau_{FWHM} = 230$ fs). These films show the thickness-dependent SA response at 400 nm [Fig. 3(b)]. The extracted I_S value decreases as the film thickness increases. However, no definite variation of I_S with pulse energy is observed [inset of Fig. 3(b)]. The magnitude of I_S is larger at 400 nm than at 800 nm, indicating that the optical absorption of these $PtSe_2$ films is easily saturated in the near-IR range than in the visible range.

Degenerate 400 nm pump-probe measurements were used to reveal the NLA process at 400 nm, and the spot sizes of the pump and probe beams focused at the samples were about 60 μm and 26 μm, respectively. As shown in Fig. 5(a), the positive ΔT/T signal around 0 delay time confirms the SA properties at 400 nm. There is no sign reversal in these time-resolved curves; thus, there is only SA in these films at any pulse repetition rate. The normalized ΔT signal of the thicker film relaxes slower [inset of Figs. 5(a) and 5(b)], confirming the stronger state-filling effect and smaller I_S value for the thicker film. The time-resolved normalized ΔT signal of these films has no definite change with the pump fluence (see S6 in the supplementary material), suggesting the insignificant influence of the hot phonon effect and the pulse energy-independent I_S value in these $PtSe_2$ films.[25,29] Therefore, for both 400 nm and 800 nm cases, the time-resolved ΔT/T spectroscopies strongly support the observed SA characteristics of these films.

An extra pump-probe measurement indicates that the relaxation time ($\tau = 346 \pm 35$ ps) of semimetallic bulk $PtSe_2$ is longer than the time constant τ_2 of sample F (not shown here). Wang *et al.* showed that the τ (I_S) of the semimetallic few layer $PtSe_2$ film is longer

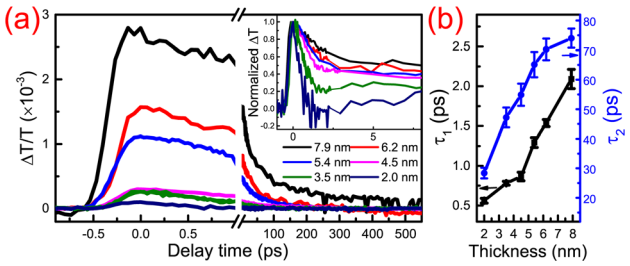

FIG. 5. (a) Time-resolved degenerate 400 nm pump-probe ΔT/T spectroscopies of $PtSe_2$ films; inset: the normalized ΔT traces around 0 delay time; the pump fluence was 0.75 mJ/cm^2. (b) The dependence of time constants on the film thickness.

(smaller) than that of the semiconducting $PtSe_2$ film.[18] More semimetallic content in the thicker $PtSe_2$ film leads to the decrease in both the carrier relaxation rate and the I_S value as the film thickness increases. Thus, the variation of both relaxation time and I_S with the film thickness originates from the accompanied change of the semimetallic content with the film thickness.

These results manifest that the direct CVD-grown $PtSe_2$ film possesses excellent SA properties with smaller I_S than its analog, multilayer black phosphorus, MoS_2 nanosheet film, and so on (see S7 in the supplementary material).[3,5–7,24–26,31] The I_S values of these $PtSe_2$ films at 800 nm are about one order of magnitude smaller than that of the TAC-fabricated $PtSe_2$ film with a similar thickness ($\sim$100 GW/cm^2).[16,18] The difference should be caused by the different component in the $PtSe_2$ films synthesized by different methods.[16]

Optical heterodyne detection of the optical Kerr effect[32] had been performed to explore the nonlinear refraction of these $PtSe_2$ films. However, no reliable nonlinear refraction signal was obtained. We had not seen a tiny self-focusing/self-defocusing induced light intensity distribution change when $PtSe_2$ was moved along the Z axis. Therefore, it is concluded that the nonlinear refractive index of these $PtSe_2$ films should not be giant (less than 1×10^{-12} cm^2/W estimated from optical Kerr effect measurements), smaller than that of TAC-fabricated $PtSe_2$ films (on the order of -2×10^{-11} cm^2/W).[18] Therefore, the NLO properties of $PtSe_2$ are related to not only the thickness but also the growth method. The thickness could be controlled in the growth process via the predeposited Pt film thickness in the TAC method and the growth time in the direct CVD method.

In summary, ultrafast NLA properties of $PtSe_2$ films, composed of both semiconducting and semimetallic phases in a single film, have been studied. These $PtSe_2$ films possess significant thickness-dependent SA at 400 nm and 800 nm. The saturation intensities at both 400 nm and 800 nm decrease with the increase in the film thickness due to the accompanied increase in the semimetallic component. Time-resolved $\Delta T/T$ spectroscopies further demonstrate the SA properties and support the dependence of saturation intensity on the film thickness. As compared with the TAC-fabricated $PtSe_2$ films, these $PtSe_2$ films exhibit pure SA with a much smaller saturation intensity and nonlinear refractive index. $PtSe_2$ provides a platform to modulate the NLA properties via the synthesis method and film thickness, which is determined in the fabrication process (i.e., not to change the $PtSe_2$ thickness after fabrication), for nonlinear photonic applications.

See the supplementary material for the details of characterization, bandgap extraction, optical nonlinearity measurements, and analysis.

This work was supported by the National Natural Science Foundation of China (Nos. 61705115, 11504265, 11504187, and 11304166), the Natural Science Foundation of Tianjin (No. 19JCQNJC01800), and the Fundamental Research Funds for the Central Universities-Nankai University (No. 63191137).

REFERENCES

[1] A. Autere, H. Jussila, Y. Dai, Y. Wang, H. Lipsanen, and Z. Sun, Adv. Mater. **30**(24), 1705963 (2018).
[2] H. Liu, A.-P. Luo, F.-Z. Wang, R. Tang, M. Liu, Z.-C. Luo, W.-C. Xu, C.-J. Zhao, and H. Zhang, Opt. Lett. **39**(15), 4591–4594 (2014).
[3] Q. Ouyang, K. Zhang, W. Chen, F. Zhou, and W. Ji, Opt. Lett. **41**(7), 1368–1371 (2016).
[4] Z. Sun, A. Martinez, and F. Wang, Nat. Photonics **10**, 227 (2016).
[5] J. Zhang, X. Yu, W. Han, B. Lv, X. Li, S. Xiao, Y. Gao, and J. He, Opt. Lett. **41**(8), 1704–1707 (2016).
[6] X. Zheng, R. Chen, G. Shi, J. Zhang, Z. Xu, X. a Cheng, and T. Jiang, Opt. Lett. **40**(15), 3480–3483 (2015).
[7] Y. Wang, G. Huang, H. Mu, S. Lin, J. Chen, S. Xiao, Q. Bao, and J. He, Appl. Phys. Lett. **107**(9), 091905 (2015).
[8] Y. Zhao, J. Qiao, Z. Yu, P. Yu, K. Xu, S. P. Lau, W. Zhou, Z. Liu, X. Wang, W. Ji, and Y. Chai, Adv. Mater. **29**(5), 1604230 (2017).
[9] A. Ciarrocchi, A. Avsar, D. Ovchinnikov, and A. Kis, Nat. Commun. **9**(1), 919 (2018).
[10] Y. Wang, L. Li, W. Yao, S. Song, J. T. Sun, J. Pan, X. Ren, C. Li, E. Okunishi, Y.-Q. Wang, E. Wang, Y. Shao, Y. Y. Zhang, H.-T. Yang, E. F. Schwier, H. Iwasawa, K. Shimada, M. Taniguchi, Z. Cheng, S. Zhou, S. Du, S. J. Pennycook, S. T. Pantelides, and H.-J. Gao, Nano Lett. **15**(6), 4013–4018 (2015).
[11] L.-H. Zeng, S.-H. Lin, Z.-J. Li, Z.-X. Zhang, T.-F. Zhang, C. Xie, C.-H. Mak, Y. Chai, S. P. Lau, L.-B. Luo, and Y. H. Tsang, Adv. Funct. Mater. **28**(16), 1705970 (2018).
[12] C. Yim, K. Lee, N. McEvoy, M. O'Brien, S. Riazimehr, N. C. Berner, C. P. Cullen, J. Kotakoski, J. C. Meyer, M. C. Lemme, and G. S. Duesberg, ACS Nano **10**(10), 9550–9558 (2016).
[13] Z. Wang, Q. Li, F. Besenbacher, and M. Dong, Adv. Mater. **28**(46), 10224–10229 (2016).
[14] J. Shi, Y. Huan, M. Hong, R. Xu, P. Yang, Z. Zhang, X. Zou, and Y. Zhang, ACS Nano **13**(7), 8442–8451 (2019).
[15] A. Kandemir, B. Akbali, Z. Kahraman, S. V. Badalov, M. Ozcan, F. Iyikanat, and H. Sahin, Semicond. Sci. Technol. **33**(8), 085002 (2018).
[16] G. Wang, K. Wang, N. McEvoy, Z. Bai, C. P. Cullen, C. N. Murphy, J. B. McManus, J. J. Magan, C. M. Smith, G. S. Duesberg, I. Kaminer, J. Wang, and W. J. Blau, Small **15**(34), 1902728 (2019).
[17] J. Yuan, H. Mu, L. Li, Y. Chen, W. Yu, K. Zhang, B. Sun, S. Lin, S. Li, and Q. Bao, ACS Appl. Mater. Interfaces **10**(25), 21534–21540 (2018).
[18] L. Wang, S. Zhang, N. McEvoy, Y.-Y. Sun, J. Huang, Y. Xie, N. Dong, X. Zhang, I. M. Kislyakov, J.-M. Nunzi, L. Zhang, and J. Wang, Laser Photonics Rev. **13**(8), 1900052 (2019).
[19] C. Yim, N. McEvoy, S. Riazimehr, D. S. Schneider, F. Gity, S. Monaghan, P. K. Hurley, M. C. Lemme, and G. S. Duesberg, Nano Lett. **18**(3), 1794–1800 (2018).
[20] J. Xie, D. Zhang, X.-Q. Yan, M. Ren, X. Zhao, F. Liu, R. Sun, X. Li, Z. Li, S. Chen, Z.-B. Liu, and J.-G. Tian, 2D Mater. **6**(3), 035011 (2019).
[21] C. Yim, V. Passi, M. C. Lemme, G. S. Duesberg, C. Ó. Coileáin, E. Pallecchi, D. Fadil, and N. McEvoy, npj 2D Mater. Appl. **2**(1), 5 (2018).
[22] B. Gompf, J. Beister, T. Brandt, J. Pflaum, and M. Dressel, Opt. Lett. **32**(11), 1578–1580 (2007).
[23] M. Hövel, B. Gompf, and M. Dressel, Phys. Rev. B **81**(3), 035402 (2010).
[24] X. Zheng, Y. Zhang, R. Chen, X. a Cheng, Z. Xu, and T. Jiang, Opt. Express **23**(12), 15616–15623 (2015).
[25] G. Xing, H. Guo, X. Zhang, T. C. Sum, and C. H. A. Huan, Opt. Express **18**(5), 4564–4573 (2010).
[26] H. Zhang, S. B. Lu, J. Zheng, J. Du, S. C. Wen, D. Y. Tang, and K. P. Loh, Opt. Express **22**(6), 7249–7260 (2014).
[27] H. Yang, X. Feng, Q. Wang, H. Huang, W. Chen, A. T. S. Wee, and W. Ji, Nano Lett. **11**(7), 2622–2627 (2011).
[28] X.-Q. Yan, F. Liu, X.-T. Kong, J. Yao, X. Zhao, Z.-B. Liu, and J.-G. Tian, J. Opt. Soc. Am. B **34**(1), 218–226 (2017).
[29] S. Wu, W.-T. Liu, X. Liang, P. J. Schuck, F. Wang, Y. R. Shen, and M. Salmeron, Nano Lett. **12**(11), 5495–5499 (2012).
[30] J. He, N. Kumar, M. Z. Bellus, H.-Y. Chiu, D. He, Y. Wang, and H. Zhao, Nat. Commun. **5**(1), 5622 (2014).
[31] S. Lu, Y. Ge, Z. Sun, Z. Huang, R. Cao, C. Zhao, S. Wen, D. Fan, J. Li, and H. Zhang, Photonics Res. **4**(6), 286–292 (2016).
[32] E. Dremetsika, B. Dlubak, S.-P. Gorza, C. Ciret, M.-B. Martin, S. Hofmann, P. Seneor, D. Dolfi, S. Massar, P. Emplit, and P. Kockaert, Opt. Lett. **41**(14), 3281–3284 (2016).